

Irradiation creep of high purity CVD silicon carbide as estimated by the bend stress relaxation method

Y. Katoh^{a,*}, L.L. Snead^a, T. Hinoki^b, S. Kondo^b, A. Kohyama^b

^a Materials Science and Technology Division, Oak Ridge National Laboratory, P.O. Box 2008, MS-6138, Oak Ridge, TN 37831-6138, USA

^b Institute of Advanced Energy, Kyoto University, Uji, Kyoto 611-0011, Japan

Abstract

The bend stress relaxation technique was applied for an irradiation creep study of high purity, chemically vapor-deposited beta-phase silicon carbide (CVD SiC) ceramic. A constant bend strain was applied to thin strip samples during neutron irradiation to fluences 0.2–4.2 dpa at various temperatures in the range ~400 to ~1080 °C. Irradiation creep strain at <0.7 dpa exhibited only a weak dependence on irradiation temperature. However, the creep strain dependence on fluence was non-linear due to the early domination of the initial transient creep, and a transition in creep behavior was found between ~950 and ~1080 °C. Steady-state irradiation creep compliances of polycrystalline CVD SiC at doses >0.7 dpa were estimated to be $2.7(\pm 2.6) \times 10^{-7}$ and $1.5(\pm 0.8) \times 10^{-6}$ (MPa dpa)⁻¹ at ~600 to ~950 °C and ~1080 °C, respectively, whereas linear-averaged creep compliances of $1\text{--}2 \times 10^{-6}$ (MPa dpa)⁻¹ were obtained for doses of 0.6–0.7 dpa at all temperatures. Monocrystalline 3C SiC samples exhibited significantly smaller transient creep strain and greater subsequent deformation when loaded along $\langle 011 \rangle$ direction.

© 2007 Elsevier B.V. All rights reserved.

1. Introduction

Silicon carbide (SiC) and its fiber-reinforced composite are emerging engineering materials for fusion and fission applications [1–6]. The potential of SiC ceramics relies on their unique combined properties such as neutron irradiation resistance, high temperature strength and inertness, low electrical conductivity, low activation/low decay heat, low tritium permeability, and low specific mass. Recent advances in SiC-based ceramic composite technol-

ogy has triggered the efforts toward practical applications of continuous SiC fiber-reinforced SiC-matrix ceramic composites (SiC/SiC composites) for fusion blanket structural and functional components [1,4] and for gas-cooled fission reactor components [5,6].

One of the most critical issues which has not yet been addressed adequately for nuclear application of SiC-based ceramics and composites is irradiation creep [7]. Irradiation creep is important not only for life-time estimation or stress-limit determination for structural applications but also for determining design limits in functional applications such as flow channel inserts in the blanket regions of fusion reactors.

* Corresponding author. Tel.: +1 865 576 5996; fax: +1 865 241 3650.

E-mail address: katohy@ornl.gov (Y. Katoh).

Previous studies on irradiation creep of SiC (-based materials) have been very limited and contradictory. Irradiation creep of chemically vapor-deposited (CVD) SiC was studied by Price in 1977 [8]. In that work, elastically bent strip samples of CVD SiC were irradiated in a fission reactor to a dose of $\sim 7.7 \times 10^{25}$ n/m² ($E > 0.18$ MeV), and the creep compliance was estimated to be $\lesssim 1 \times 10^{-6}$ (MPa dpa)⁻¹ over the 780–1130 °C temperature range. Scholz and co-workers [9–12] measured the creep deformation of SCS-6 CVD SiC-based fiber, which was loaded to a constant torsional shear stress under penetrating proton or deuteron beam irradiation. They reported several important observations including the linear stress and flux dependency at 600 °C of the tangential creep rate at ~ 0.06 dpa, and an approximate irradiation creep compliance of $> 1 \times 10^{-5}$ (MPa dpa)⁻¹, which was only weakly and non-monotonically dependent on irradiation temperature over the range 450–1100 °C.

The adopted experimental method and setup in the Scholz work are reliable. However, the determined creep compliance was ~ 50 times larger at ~ 800 °C than reported by Price [8]. Moreover, the CVD SiC fiber used by Scholz is known to exhibit anomalous thermal creep behavior presumably due to excess silicon on grain boundaries [13]. The purpose of the present work is to better define the irradiation creep compliance of high purity, stoichiometric CVD SiC in a series of controlled fission reactor irradiations using the bend stress relaxation (BSR) technique.

2. Experimental procedures

The BSR technique was established by Morscher and DiCarlo to evaluate the thermal creep behavior of ceramic fibers [14]. In a BSR irradiation creep experiment, thin fiber or strip samples are constrained to a fixed bend radius R_0 during irradiation at temperature T and damage rate ϕ for a period t . The bend stress relaxation ratio (BSR ratio, m) is defined by

$$m(\phi, T, t) = \frac{\sigma_a}{\sigma_0} = \frac{E_a}{E_0} \left(1 - \frac{R_0}{R_a} \right), \quad (1)$$

where σ_0 and σ_a are the initial and the final bend stresses, E_0 and E_a are the non-irradiated and irradiated Young's moduli, respectively, and R_a is the unconstrained bend radius after irradiation. Assuming a linear stress dependence of the steady-state

irradiation creep rate ($\dot{\epsilon}_{ic}$) and no transient creep contribution, $\dot{\epsilon}_{ic}$ is often expressed by

$$\dot{\epsilon}_{ic}/\sigma \approx B\phi = B_0\phi + D\dot{S}, \quad (2)$$

where B and B_0 are the apparent and swelling-free irradiation creep compliances, \dot{S} is swelling rate, and D is creep-swelling coupling coefficient [15]. Ignoring the swelling term, B can be derived by the following equation:

$$B = \frac{\ln(m_1/m_2)}{E\phi(t_2 - t_1)} \quad (3)$$

using m values at two different dose levels.

Compared to the conventional experimental techniques for irradiation creep studies such as the pressurized tube creep and externally loaded in-pile tensile or compressive creep techniques, the BSR technique requires only very small specimens in a simple geometry. However, the successful application of BSR technique to irradiation creep study of bulk ceramics hinges upon preparation of thin strip samples with sufficient flexural strength and the appropriate design of specimen holders that ensure good thermal contact with the specimens without imposing undesired friction or chemical interactions.

For the first set of experiments, thin strip samples with dimensions of 25 or 40 mm \times 1 mm \times 50 μ m were prepared. Materials used were high purity 'CVD SiC' manufactured by Rohm and Haas Co., Advanced Materials (Waborn, Massachusetts, USA), and a free-standing monocrystalline wafer of '3C SiC' with {100} surface orientation provided by Hoya Advanced Semiconductors Technologies, Inc. (Tokyo, Japan). The monocrystalline specimens were machined so that the longitudinal direction was parallel with one of the {011} orientations. The specimens after finish-grinding exhibited typical flexural strength of ~ 400 MPa. The materials tested are summarized in Table 1.

The specimen holder was designed to retain the thin strip samples in a narrow gap with a curvature of 100 mm radius. Holders were made from CVD SiC and HexoloyTM SA to avoid potential chemical interactions with the SiC specimens during irradiation. The combination of the present specimen thickness and the curvature gave the initial bend stresses on the order of 100 MPa. The bend radii for individual specimens were determined by measuring the differential tangential angles at both ends of the sample strips before (constrained) and after (unconstrained) irradiation. The accuracy of bend

Table 1
List of materials used in this work

Material	Crystal structure	Manufacturer	Density (g/cm ³)	Purity (%)
CVD SiC	Polycrystalline beta	Rohm and Haas	3.21	>99.9995
3C SiC	Monocrystalline beta	Hoya	3.21	~99.99 ^a

^a Doped nitrogen as major impurity.

Table 2
Summary of irradiation conditions and result of BSR irradiation creep experiment

Material	T_{irr} , °C	Fluence, dpa	Reactor	Initial/final bend stress, MPa	Initial/final bend strain, $\times 10^{-4}$	Creep strain, $\times 10^{-4}$	BSR ratio m	Average creep compliance, $\times 10^{-6}$ (MPa dpa) ⁻¹
CVD SiC	400	0.6	JMTR	82/60	1.80/1.39	0.41	0.77	0.97
	600	0.2	JMTR	81/57	1.80/1.31	0.49	0.73	3.5
		0.6	JMTR	81/46	1.80/1.05	0.75	0.58	2.0
	640	3.7	HFIR	87/36	1.95/0.83	1.12	0.42	0.50
	700	0.7	HFIR	102/72	2.27/1.64	0.63	0.72	1.1
	750	0.6	JMTR	80/55	1.80/1.27	0.53	0.71	1.3
	1030	0.7	HFIR	86/61	1.94/1.42	0.52	0.73	0.97
	1080	4.2	HFIR	101/8	2.29/0.19	2.10	0.08	0.91
3C SiC	640	3.7	HFIR	87/30	1.94/0.68	1.26	0.35	0.59
	700	0.7	HFIR	102/90	2.27/2.06	0.21	0.87	0.34
	1030	0.7	HFIR	86/57	1.94/1.31	0.63	0.67	1.2
	1080	4.2	HFIR	101/1	2.29/0.02	2.27	0.01	1.1

angle measurement by optical microscopy was $<0.1^\circ$, which gives $<1\%$ error in determination of the BSR ratios, m .

The irradiation was performed in the High Flux Isotope Reactor (HFIR), Oak Ridge National Laboratory (Oak Ridge, Tennessee, USA) and in the Japan Atomic Materials Test Reactor (JMTR), Japan Atomic Energy Agency (Oarai, Japan) to a maximum neutron fluence of 4.2×10^{25} n/m² ($E > 0.1$ MeV). An equivalence of one displacement per atom (dpa) = 1×10^{25} n/m² ($E > 0.1$ MeV) is assumed hereafter based on damage calculations given elsewhere [16]. The nominal irradiation temperatures were 640–1080 °C for HFIR, and 400, 600, and 750 °C for JMTR. Two polycrystalline samples and one monocrystalline sample were irradiated in each condition in HFIR, whereas 4–6 polycrystalline samples were irradiated in JMTR. Details of the irradiation conditions are summarized in Table 2.

3. Results

The results of the strain measurement are summarized in Table 2. The strain and stress values are the maximum that occur on the tensile and com-

pressive surfaces of bent specimens. The creep strain corresponds to the unconstrained final residual strain, and the final elastic strain was determined by subtracting the creep strain from the initial elastic strain. The initial and the final bend stresses were determined using temperature-dependent Young's modulus data for non-irradiated CVD SiC [17]. The linear-averaged irradiation creep compliances, \bar{B} , were derived by dividing the creep strain by the product of fluence and the linear-averaged stress. The irradiation effect on Young's modulus was neglected in this work, and may impose a few percent error to \bar{B} [18].

The irradiation-creep BSR ratios are plotted as a function of irradiation temperature and neutron fluence in Figs. 1 and 2, respectively. The error bars correspond to the maximum cumulative uncertainty associated with the BSR ratio determination. The specimen-to-specimen variations of BSR ratios were within ± 0.02 for the HFIR-irradiated CVD SiC. The larger error for the JMTR data points was caused by the limited resolution in optical images of the pre-irradiation specimens constrained in holder assemblies.

The obvious features in Figs. 1 and 2 are (1) the general lack of temperature dependence at

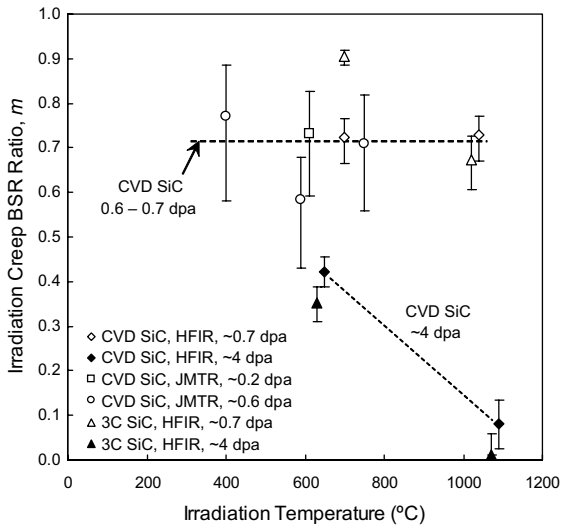


Fig. 1. Bend stress relaxation ratios for the irradiated polycrystalline ('CVD SiC') and monocrystalline ('3C SiC') vapor-deposited beta-phase SiC, as a function of irradiation temperature.

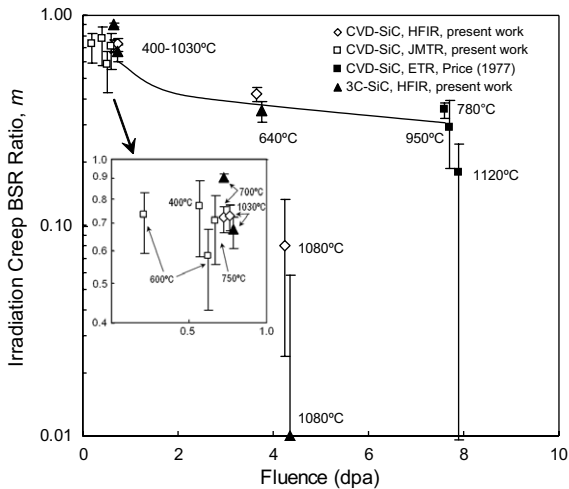


Fig. 2. Neutron fluence dependence of irradiation creep BSR ratio. Note that slope is proportional to irradiation creep compliance.

≤ 0.7 dpa, (2) significantly larger creep deformation at $\sim 1080^{\circ}\text{C}$ than at $\sim 640^{\circ}\text{C}$ at ~ 4 dpa, (3) a reasonable agreement between data from HFIR and JMTR, and (4) slight difference between polycrystalline 'CVD SiC' and monocrystalline '3C SiC' samples at ~ 640 to $\sim 700^{\circ}\text{C}$. A slightly negative correlation between the BSR ratio and irradiation temperature could be noticed, but the temperature effect does not appear significant compared to the

error bars shown. In Fig. 2, irradiation creep BSR ratios calculated from data published by Price [8] are plotted together. From Eq. (3), the slope of the fitted curve in Fig. 2 is proportional to B . Those data do not indicate constant creep compliances but instead a rather steep stress relaxation before a dose of 0.2 dpa is achieved, and the initial stress relaxation dominates the total stress relaxation at doses ≤ 0.7 dpa.

4. Discussion

The \bar{B} values, which have been obtained by taking $t_1 = 0$ and $m_1 = 1$ in Eq. (3), are inappropriate for predicting the long-range irradiation creep behavior of SiC, as obvious in Fig. 2. For the light-ion irradiated SCS-6 fiber, Scholz et al. report domination of the primary transient creep until at least 0.05 dpa for $< 800^{\circ}\text{C}$ [12]. They attributed the primary transient creep behavior to anisotropic partitioning of point defects in association with the rapid interstitial cluster formation, by correlating the transient creep rate with the swelling rate of SiC estimated for the relevant temperatures [12]. The fluence dependence of the BSR ratio observed at 600°C in this work supports the early domination of transient irradiation creep. Although it is not clear from Fig. 2 if the fluence of ~ 0.7 dpa at 600 – 750°C is still within the transient creep regime or not, the BSR ratios similar to that at 0.2 dpa suggest that the material is close to the end of the transient creep regime by ~ 0.7 dpa. The near-saturation of swelling at < 1 dpa in this temperature range [19] also supports this assertion, assuming the correlation of irradiation creep and low-temperature swelling. Meanwhile, Eq. (2) also assumes the linear dependence of irradiation creep rate on the stress magnitude and neutron flux. The assumptions of linear stress and flux dependence may be adequate because of the light-ion data reported by Scholz et al. [9] and existing irradiation creep models, but will have to be confirmed by neutron irradiation in future work.

Based on the discussion above, it is possible that a steady-state irradiation creep is nearly achieved by ~ 0.6 dpa. By assuming so, $B = 2.7(\pm 2.6) \times 10^{-7} (\text{MPa dpa})^{-1}$ can be derived. Fig. 2 shows that the BSR ratios at 3.7 dpa and $\sim 640^{\circ}\text{C}$ in this work and at 7.7 dpa and ~ 780 and $\sim 950^{\circ}\text{C}$ in the Price work are comparable, suggesting even smaller steady-state creep compliance values may be realistic at these temperatures. On the other hand,

Fig. 2 also indicates that there likely exists a major transition in irradiation creep behavior between $\sim 950^\circ\text{C}$ and $\sim 1080^\circ\text{C}$, and $B = 1.5(\pm 0.8) \times 10^{-6} (\text{MPa dpa})^{-1}$ is derived for $\sim 1080^\circ\text{C}$ irradiation assuming that the transition to steady-state has occurred at a similar dose. On the other hand, linear-averaged irradiation creep compliances of $1\text{--}2 \times 10^{-6} (\text{MPa dpa})^{-1}$ were obtained for dose range 0 to 0.7 dpa at all temperatures, indicating the possibly large quantitative effect of transient creep processes. The obtained compliance values are plotted in Fig. 3, along with the linear-averaged irradiation creep compliance values from the work by Price [8], and the low dose light-ion creep compliance values published by Scholz [12]. The very large compliance values for the light-ion irradiation creep are believed to be primarily due to the fact that they represent tangential compliances within the low dose transient creep regime, whereas the presumably higher surviving defect efficiency by light ions, the non-stoichiometric grain boundary chemistry, and the shear stress in preferred circumferential crystallographic orientation in SCS-6 fiber might have contributed as well.

The estimated irradiation creep compliance value for SiC irradiated at $\sim 1080^\circ\text{C}$ is close to the typical values for neutron-irradiated metals and alloys, while it is by about an order of magnitude greater than the estimated steady-state SiC value for

$< \sim 950^\circ\text{C}$ irradiation. This temperature of the irradiation creep transition approximately corresponds to the transition temperature of irradiated microstructures in SiC from black-spot type ultra-fine defects to better-defined Frank faulted loops [20]. Moreover, it also likely coincides with the onset temperature for significant vacancy mobility and void swelling in neutron-irradiated SiC [21]. Therefore, it is conceivable that the point defect partitioning in favor of stress relaxation effectively operates in SiC at $\sim 1080^\circ\text{C}$ or higher temperatures during the steady-state creep regime, in more or less similar ways as in metals and alloys. A recent ion irradiation study by Kondo et al, in which stress-induced anisotropy of interstitial-type Frank loop microstructure was observed in SiC, supports this implication [22]. Operation of the conventional irradiation creep mechanisms should be severely retarded in SiC at $< \sim 950^\circ\text{C}$ due to the very limited vacancy mobility and the sink effect of the ultra-fine clusters.

The observed difference in stress relaxation behavior between the polycrystalline and monocrystalline materials involves several complexities. At 0.7 dpa and $\sim 700^\circ\text{C}$, the BSR ratio for the monocrystalline sample was clearly greater than the polycrystalline sample, implying greater transient creep strain for the polycrystals. On the other hand, at 3.7 dpa and $\sim 640^\circ\text{C}$, the monocrystalline sample exhibits a smaller BSR ratio, implying a greater creep rate after 0.7 dpa. At $\sim 1030^\circ\text{C}$ and $\sim 1080^\circ\text{C}$, the monocrystalline samples exhibited slightly smaller BSR ratios than the polycrystalline samples, although the difference may not be significant.

Possible explanations for the difference in irradiation creep between the polycrystalline and monocrystalline samples at ~ 640 to $\sim 700^\circ\text{C}$ include (1) crystallographic orientation effect, (2) crystallographic texture effects in polycrystals, and (3) the influence of as-grown defects. Although a significant difference in average resolved shear stress on $\{111\}$ planes is not anticipated in the present experiment, crystallographic orientation effect may not be disproved because of the fact that microstructures in SiC irradiated at $< 800^\circ\text{C}$ comprise ultra-fine point defect clusters of unknown configurations [20]. The texture effect could also have contributed to retard the crystallographic orientation-dependent deformation of the polycrystalline SiC. The effect of as-grown defects could be a reason for the less significant transient irradiation creep in monocrystalline SiC.

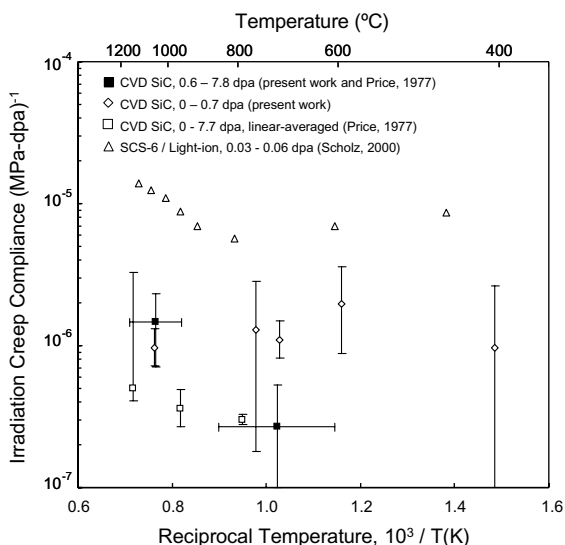


Fig. 3. Irradiation creep compliance of chemically vapor deposited SiC and SiC-based materials estimated by various experiments. Note that substantial uncertainty in irradiation temperature is present for the Price data points.

5. Conclusions

Irradiation creep strain for high purity, polycrystalline CVD SiC exhibited weak temperature dependence at <0.7 dpa in the ~400 to ~1030 °C temperature range, whereas a major transition at higher doses likely exists between ~950 °C and ~1080 °C. The creep strain appeared highly non-linear with neutron fluence due to the early domination of the transient irradiation creep. The transient creep was speculated to have been caused by the rapid development of defect clusters and the structural relaxation of as-grown defects during early stages of irradiation damage accumulation. At ~1080 °C, irradiation creep mechanisms which are common to metals are likely operating. Steady-state irradiation creep compliances for CVD SiC were estimated to be $2.7(\pm 2.6) \times 10^{-7}$ and $1.5(\pm 0.8) \times 10^{-6} (\text{MPa dpa})^{-1}$ at ~600 to ~950 °C and ~1080 °C, respectively, whereas linear-averaged creep compliances of $1\text{--}2 \times 10^{-6} (\text{MPa dpa})^{-1}$ were obtained for doses of 0.6–0.7 dpa at all temperatures. Monocrystalline 3C SiC samples exhibited significantly smaller transient creep strain by 0.7 dpa and greater subsequent deformation when loaded along $\langle 011 \rangle$ direction.

For better defining the irradiation creep behavior of SiC and the underlying physical mechanisms, it will be essential to further examine the stress dependence, dose dependence, effect of crystallographic orientation, microstructures of the crept samples, and the coupling between irradiation creep and low-temperature swelling.

Acknowledgements

This research was sponsored by the Office of Fusion Energy Sciences, US Department of Energy under contract DE-AC05-00OR22725 with UT-Battelle, LLC., JUPITER-II Japan-US collaboration on fusion blanket systems and materials,

and US Department of Energy Nuclear Energy Research Initiative Program NERI-2002-131.

References

- [1] Y. Katoh, L.L. Snead, C.H. Henager, A. Hasegawa, A. Kohyama, B. Riccardi, J.B.J. Hegeman, *J. Nucl. Mater.*, in press, doi:10.1016/j.jnucmat.2007.03.032.
- [2] S.J. Zinkle, *Fus. Sci. Technol.* 47 (2005) 821.
- [3] R. Naslain, *Compos. Sci. Technol.* 64 (2004) 155.
- [4] M. Abdou, D.-K. Sze, C. Wong, M. Sawan, A. Ying, N.B. Morley, S. Malang, *Fus. Sci. Technol.* 47 (2005) 475.
- [5] W.R. Corwin, T.D. Burchell, W.G. Halsey, G.O. Hayner, Y. Katoh, J.W. Klett, T.E. McGreevy, R.K. Nanstad, W. Ren, L.L. Snead, R.E. Stoller, D.F. Wilson, Updated Generation IV Reactors Integrated Materials Technology Program Plan, Revision 2, ORNL/TM-2003/244/R2, Oak Ridge National Laboratory, 2005.
- [6] A. Kohyama, T. Hinoki, T. Mizuno, T. Kunugi, M. Sato, Y. Katoh, J.S. Park. in: Proceedings of 2005 International Congress on Advances in Nuclear Power Plants (ICAPP-05), 2005.
- [7] A.R. Raffray, R. Jones, G. Aiello, M. Billone, L. Giancarli, H. Golfier, A. Hasegawa, Y. Katoh, A. Kohyama, S. Nishio, B. Riccardi, M.S. Tillack, *Fus. Eng. Des.* 55 (2001) 55.
- [8] R.J. Price, *Nucl. Technol.* 35 (1977) 320.
- [9] R. Scholz, *J. Nucl. Mater.* 258–263 (1998) 1533.
- [10] R. Scholz, *J. Nucl. Mater.* 254 (1998) 74.
- [11] R. Scholz, G.E. Youngblood, *J. Nucl. Mater.* 283–287 (2000) 372.
- [12] R. Scholz, R. Mueller, D. Lesueur, *J. Nucl. Mater.* 307–311 (2002) 1183.
- [13] J.A. DiCarlo, *J. Mater. Sci.* 21 (1986) 217.
- [14] G.N. Morscher, J.A. DiCarlo, *J. Am. Ceram. Soc.* 75 (1992) 136.
- [15] K. Ehrlich, *J. Nucl. Mater.* 100 (1981) 149.
- [16] H.L. Heinisch, L.R. Greenwood, W.J. Weber, R.E. Williford, *J. Nucl. Mater.* 327 (2004) 175.
- [17] Y. Katoh, L.L. Snead, *J. ASTM Int.* 2 (2005) 12377.
- [18] Y. Katoh, L.L. Snead, *Ceram. Eng. Sci. Proc.* 26 (2005) 265.
- [19] Y. Katoh, H. Kishimoto, A. Kohyama, *J. Nucl. Mater.* 307 (2002) 1221.
- [20] Y. Katoh, N. Hashimoto, S. Kondo, L.L. Snead, A. Kohyama, *J. Nucl. Mater.* 351 (2006) 228.
- [21] L.L. Snead, Y. Katoh, S. Connery, *J. Nucl. Mater.*, in press, doi:10.1016/j.jnucmat.2007.03.097.
- [22] S. Kondo, A. Kohyama, T. Hinoki, *J. Nucl. Mater.*, in press, doi:10.1016/j.jnucmat.2007.03.085.